ORIGINAL ARTICLE
DOI: https://doi.org/10.30932/1992-3252-2023-21-4-2

World of Transport and Transportation, 2023,
Vol. 21, Iss. 4 (107), pp. 158–166

Possibility of Monitoring the Dynamic Impact of the Rolling Stock on the Track Superstructure Using Strain Gauges and Vibrometry

Aleksandr S. ADADUROV

Victor N. FEDORININ

Sergey A. BEKHER

Mikhail A. GULYAEV

Aleksandr S. Adadurov[1], Victor N. Fedorinin[2], Sergey A. Bekher[3], Mikhail A. Gulyaev[4]

[1] VNIIZHT-Engineering Ltd., St. Petersburg, Russia.
[2] Branch of the Rzhanov Institute of Semiconductor Physics of the Siberian Branch of the Russian Academy of Sciences, Novosibirsk, Russia.
[3, 4] Siberian State Transport University, Novosibirsk, Russia.
✉ *[3] behers@mail.ru.*

ABSTRACT

One of the priority tasks in development of railway transport is to raise its efficiency by increasing the time between repairs for both the track superstructure and the rolling stock. Solving this problem is impossible without timely, complete, and reliable information about the dynamics of interaction of the rolling stock with the infrastructure. To organise monitoring of dynamic processes, completely different types of primary transducers are used: resistance strain gauges, fibre-optic sensors, dynamometers (force sensor pads), accelerometers, acoustic emission sensors. This implies relevance of the scientific and technical problem of comparative testing of sensors of different types to assess the information content of their signals and justify the criteria for choosing primary transducers when solving specific monitoring problems.

The objective of the study is to comparatively test removable resistive strain sensors, optical polarisation strain sensors and accelerometers under a passing train and to evaluate their information content to control rail depression and detect defects on the running surface of wagon wheels.

The study using finite element modelling and a physical model of a rail as of a beam on an elastic foundation, substantiates the relationship between longitudinal deformations and vertical accelerations of the rail foot. Comparative tests of removable strain-resistive and optical polarisation strain sensors and accelerometers were held on an experimental section of track under a passing train. A signal processing algorithm has been developed and the equivalence of strain gauges and vibrometers for determining the depression of a rail under a passing train has been proven. A comparison has been made of the pulse components of the signals of deformation and vibration acceleration during movement of a wheel with a defect on the running surface, and the requirements for the frequency characteristics of the sensors and their mounting on the rail surface have been substantiated.

Keywords: railways, wheel and rail dynamics, rail deformation, strain gauge, vibrometry, removable strain gauge, optical polarisation sensor, accelerometer.

Funding: the work was partially supported by state budget funds under state assignment No. 3.2023-GZ. EGISU NIOTKR [single state information system of records of R&D] registration number 123063000030–0.

For citation: Adadurov, A. S., Fedorinin, V. N., Bekher, S. A., Gulyaev, M. A. Possibility of Monitoring the Dynamic Impact of the Rolling Stock on the Track Superstructure Using Strain Gauges and Vibrometry. World of Transport and Transportation, 2023, Vol. 21, Iss. 4 (107), pp. 158–166. DOI: https://doi.org/10.30932/1992-3252-2023-21-4-2.

The text of the article originally written in Russian is published in the first part of the issue.
Текст статьи на русском языке публикуется в первой части данного выпуска.

INTRODUCTION

The dynamics of interaction between rolling stock wheels and rails [1–4] determines the reliability and service life of wagon running gear [5, 6] and elements of the track superstructure [7]. An increased level of dynamic forces in the «wheel–rail» system increases the likelihood of formation of fatigue defects and the rate of development of mechanical wear [8–10]. Excessive forces from rolling stock onto the track can lead to destruction of the rail due to defects, the dimensions of which do not exceed the detection threshold of standard ultrasonic flaw detection equipment [11–13]. For example, in 2022 alone, on the West Siberian Railway, 17 rail fractures occurred due to cracks, all of which had smaller dimensions than the maximum ones, which had not allowed them to be detected either by mobile flaw detection equipment or by removable flaw detectors. In eight cases, destruction occurred along cracks in the foot tips, which did not cross the vertical plane of symmetry of the rail and were not detected by ultrasonic testing.

One of the indicators of the dynamic impact of rolling stock on the track according to GOST [Russian state standard] 34759–2021 refers to longitudinal stresses in the flange tips, which during certification tests should not exceed 240 MPa. An increased level of stress in the foot is associated with depression of the rail in the vertical plane under a passing train, which directly affects the likelihood of brittle failure of an object with a transverse crack.

Technical condition of rolling stock on the railways of the Russian Federation and abroad is widely monitored with the Pauk [Spider], Neva, WILD, WCM, Lasca, and Atlas-LG systems [14]. These stationary rolling stock diagnostic tools monitor the levels of dynamic stress, depression, and vibration of the rails under a passing train. The advantage of this approach is the ability to classify rolling stock defects not by size and type, but directly by the degree of their negative impact on the track.

Traditionally, to control mechanical stresses and depression, the relative deformations of the rail under a passing train are measured [15–18]. The complexity of organising this type of control is associated with the laboriousness of attaching strain gauges directly to the rail using glue. At the same time, the results of deformation measurements strongly depend on installation conditions and human factors. The use of welding to attach strain gauges to rails is possible only after certification tests. All this significantly limits the possibility of quickly changing the location or scheme of measuring deformations.

Relevant is the development of removable strain sensors that provide registration of dynamic processes in rails at frequencies up to (10–20) kHz [19–23]. To increase the reliability and information content of the control process, vibrometry tools, which are accelerometers, can additionally be used. Using the example of diagnostics of bridge spans, work [24] showed that the combined use of strain gauging and vibrometry makes it possible to compensate for limitations of each method, increasing their scope of application and reliability of the results.

The *objective* of the study is to assess the possibility and to compare the results of strain gauging of rails using removable strain gauge sensors and optical polarisation sensors with the results of vibrometry under a passing train to monitor rail depression and detect defects in the running surface of railway wheels.

RESULTS

Experimental Equipment and Test Methods

Three different types of digital removable strain gauges were used to monitor strain: two strain-resistive and one optically polarisation sensor. The sensitive elements in the strain gauges were film strain gauges 2FKP-5–200-A-12-S with a base of 5 mm, a resistance of 200 Ohms and an average strain sensitivity of 2,04. The strain gauges were glued to an elastic element of a string type made of ABS plastic (Pic. 1 *a*) and of a cantilever type (beam) made of D16A duralumin (Pic. 1 *b*) using cyanoacrylate glue. The elastic elements were attached to the rail by two disk (ring) magnets with a pressing force of 10 N. The mass of the plastic sensor assembly was of 26 g, the mass of the duralumin sensitive element was of 62 g.

A string-type strain gauge (Pic. 1 *a*) with single strain gauge was connected to the «Dynamika-3» strain gauge system, registered in the state register of measuring instruments under No. 66938-17, according to the «single strain gauge» scheme with a sampling frequency of 16 kHz. The cantilever type strain gauge (Pic. 1 *b*) used four strain gauges connected via a bridge circuit to the original strain gauge device, with a sampling frequency of 4 kHz. The values of the smallest digit of the recorded digital signals were of $1{,}85 \cdot 10^{-6}$ and $1{,}7 \cdot 10^{-6}$ relative deformations, respectively.

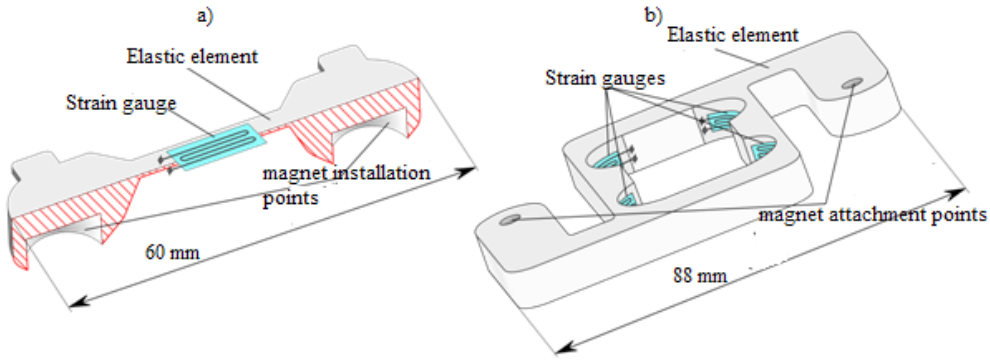

Pic. 1. Designs of removable strain gauges of string (a) and beam (b) types [performed by the authors].

Pic. 2. Appearance of the optical polarisation sensor [photo made by the authors].

In the optical polarisation sensor, an elastic element with a 60 mm base made of 12X18H10T steel transmits rail deformations to a quartz glass disk. The operating principle of the sensor is based on the phenomenon of photoelasticity and is described in detail in [25]. The value of the smallest digit of the analogue-to-digital converter in relative units of deformation was of $5 \cdot 10^{-8}$. The mass of the sensor was of 94 g.

Strain gauges were installed in inter-sleeper spaces on the lower surface of the rail foot in the symmetry plane and were oriented to measure longitudinal deformations ε_z (Pic. 3). Vibration acceleration was measured with a three-axis accelerometer based on the ADXL326 chip with an upper limit of the transmission frequency of 1600 Hz. The developed and manufactured measuring circuit ensured the conversion of acceleration into a digital signal with a sampling frequency of 12 kHz and a value of the smallest digit of $3 \cdot 10^{-3}$ m/s^2, the root-mean-square deviation of the intrinsic noise of the measuring path did not exceed $6 \cdot 10^{-2}$ m/s^2. The accelerometer was installed on the rail foot to record only one vertical component of vibration acceleration a_y (Pic. 3).

Finite element Modelling

A 7 m long rail model was divided into tetragonal elements with edge lengths from 10 to 245 mm (Pic. 3). Sleepers within a stress-strain diagram of 2000 pcs/km were reproduced by elastic boundary conditions with vertical rigidity distributed along the foot of the rail at the point of contact with the sleepers. In model experiments, the rigidity varied within the range from 10 to 200 MN/m^3. The foot tips were rigidly fixed at the rails' edges. A force from the wheel Q = 10 kN was applied to the rail head along the normal in the symmetry plane. The longitudinal deformations of the foot $\boldsymbol{\varepsilon}_z$ and the vertical displacements of the foot of the rail $\boldsymbol{\Delta}_y$ obtained by the finite element method for a rigidity of 10 MN/m^3 are presented in Pic. 4 *a, c*, for a rigidity of 100 MN/m^3 in Pic. 4 *d, e*.

Analytical Model

According to the theory of resistance of materials, a rail is a beam lying on an elastic foundation [26]. In this model, there is a relationship between the movements of the rail in the vertical plane along the *y* axis with the longitudinal deformations ε_z of the rail (Pic. 3). For a beam, the following relationship between the deflection $\Delta_y(z)$ and the bending moment $M_x(z)$ is valid:

$$E \cdot J_x \cdot \frac{d^2\Delta_y(z)}{dz^2} = M_x(z), \qquad (1)$$

where E – modulus of elasticity, MPa; J_x – section moment of inertia, m^4; $\Delta_y(z)$ and $M_x(z)$ – functions

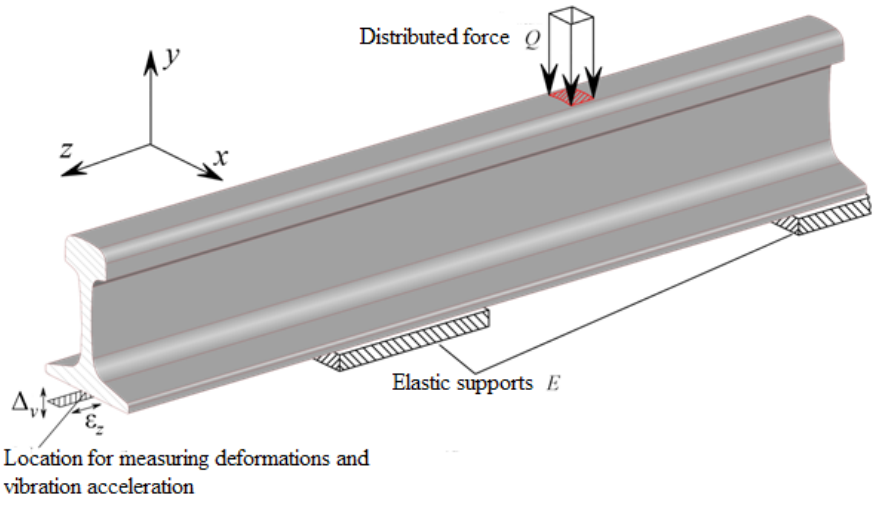

Pic. 3. Rail model for finite element calculations [performed by the authors].

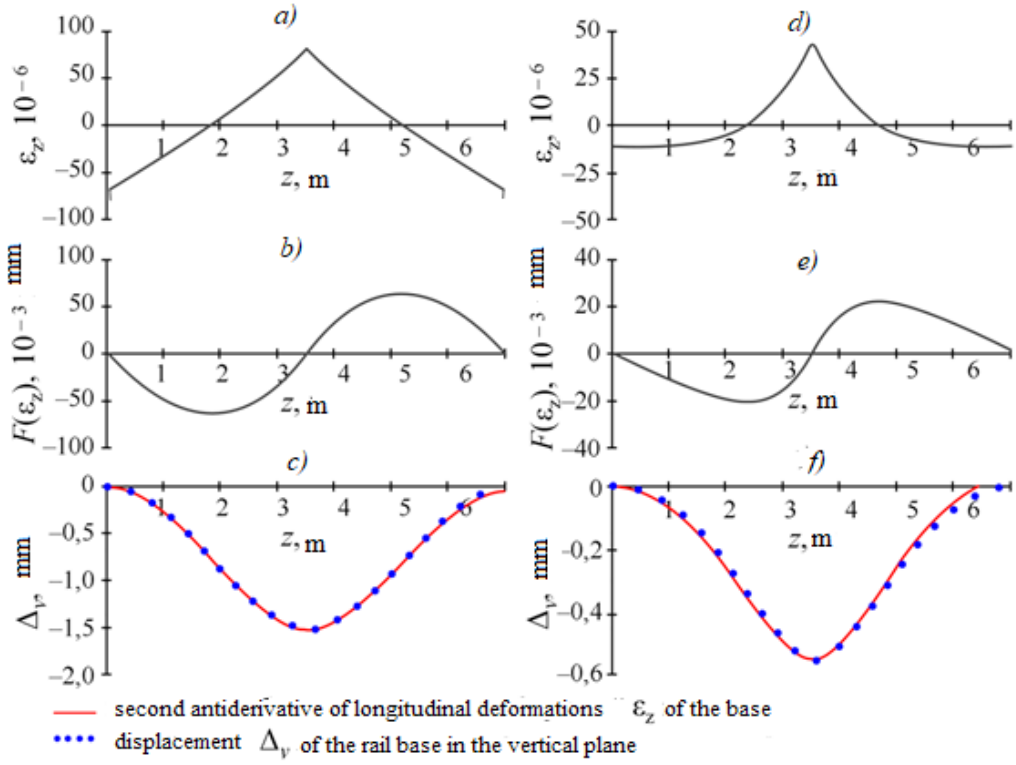

Pic. 4. Results of modelling by the finite element method of a rail with a base stiffness of 10 (a, b, c) and 100 MN/m³ (d, e, f): deformation ε_z (a, d), antiderivative of deformations $F(\varepsilon_z)$ (b, e), second antiderivative of deformations and displacement of the rail foot Δ_y (c, f) [performed by the authors].

of beam depression and of bending moment from coordinate z, m and N•m, respectively.

The bending moment creates proportional mechanical stresses in the longitudinal direction:

$$\sigma_z(z) = \frac{M_x(z)}{J_x} \bullet y_{\max}, \quad (2)$$

where $y_{\max}$ – maximum distance to the deformation measurement point from the neutral axis of the rail, m.

Combining (1) and (2) and taking into account the relationship between elastic deformations and mechanical stresses $\sigma = \varepsilon \bullet E$:

$$\frac{d^2 \bullet_y(z)}{dz^2} = \frac{\varepsilon_z}{y_{\max}}. \quad (3)$$

Expression (3) includes only geometric quantities that establish the relationship between rail depression curvature. Consequently, the pattern described by this expression, to a first approximation, does not depend either on the mechanical characteristics, or on the method of applying forces or their values, or on the boundary conditions of the rail fastening.

The beam depression function can be obtained by double integration of expression (3):

$$\Delta_y(z) = k \bullet \int_0^z \left(\int_0^u \varepsilon_z(v) dv \right) du = k \bullet F\left(F\left(\varepsilon_z(z)\right)\right), \quad (4)$$

where F – antiderivative, $k = 1/y_{max}$ – proportionality factor, m^{-1}.

To check the analytical dependences (4), the deformations ε_z (Pic. 4 *a, d*) were numerically integrated twice. The antiderivatives $F(\varepsilon_z(z))$ are shown in Pic. 4 *b, e*. The second antiderivatives of deformations $F(F(\varepsilon_z(z)))$ are shown in Pic. 4 *c, f* and coincide with the vertical movements of the foot Δ_y with an error of no more than 1 % near the point of application of the force in the area with coordinates from 1,5 to 5,5 m. The calculated proportionality coefficient $k = (12{,}5 \pm 0{,}2)\ m^{-1}$ is practically independent of stiffness in the range from 10 to 200 MN/m^3. The obtained value of coefficient k corresponds to the distance from the foot to the neutral axis of the rail $y_{max} = 0{,}08$ m (standard height of the new rail is 0,18 m).

When a train moves at a constant speed, the coordinate of the point of measurement of deformations relative to the train is described by the simplest equation:

$$z = V \bullet t, \quad (5)$$

where V is train speed, m/s.

The transition in (4) from integration over coordinate z to integration over time t can be carried out by replacing the variable in (5):

$$\Delta_y(t) = \frac{V^2}{y_{\max}} \bullet F\left(F\left(\varepsilon_z(t)\right)\right). \quad (6)$$

A similar expression can be obtained for accelerometer signals, since displacement obviously represents the second antiderivative of acceleration:

$$\Delta_y(t) = F\left(F\left(a_y(t)\right)\right), \quad (7)$$

where $a_y(t)$ is vibration acceleration of the rail foot at the moment t, m/s^2.

Expressions (6) and (7) in integral form establish a connection between the longitudinal deformations of the rail base ε_z and the vertical acceleration a_y, which, in a certain sense, indicates the equivalence of these two types of measurements:

$$\frac{V^2}{y_{\max}} \bullet F\left(F\left(\varepsilon_z(t)\right)\right) = F\left(F\left(a_y(t)\right)\right). \quad (8)$$

Expression (8) was obtained under the conditions of neglecting the uneven distribution of under-rail stiffness and is obviously determined with an accuracy of up to a certain polynomial of the first degree. In practice, expression (8) establishes a relationship between deformations and accelerations only in the low-frequency region, since double integration is a high-pass filter. The validity of equation (8) for real signals will make it possible in the future to justify the possibility of reducing the number of types of sensors installed on rails and to focus on methods for processing their signals.

Experimental Results

Experimental studies were carried out on an operating straight section of continuous track with rails of R65 type on a ballast base. Deformations of the rail foot were recorded when cargo trains were moving at speeds from 40 to 60 km/h before entering the wagon maintenance station. As the train moved along the measuring section, vibration accelerations and longitudinal deformations of the rail foot were recorded (Pic. 5).

High-frequency oscillations predominate in the accelerometer signals (Pic. 5); the passage of a wheel over the sensor installation location causes an increase in the root-mean-square deviation of the vibrations. The foot deformation reaches zero level in the middle of the wagon, when all the wheels are located as far as possible from the deformation measurement point. As the wheel approaches the strain gauge, the rail bends downwards, and longitudinal tensile stresses arise in the foot. Between the wheels and wagons, the curvature of the rail changes sign, the centre of the inscribed circle is located at the bottom, and compressive stresses are observed in the foot. The maximum value of stresses in-between wagons is 2–4 times higher than the stress between wheelsets of one bogie, the level of tensile stresses under the wheel in absolute value is 3–4 times higher than the maximum level of compressive stresses.

Significant differences in the shape of the signals (Pic. 5) of the optical polarisation sensor from the signals of the strain gauges are associated with their different locations along the

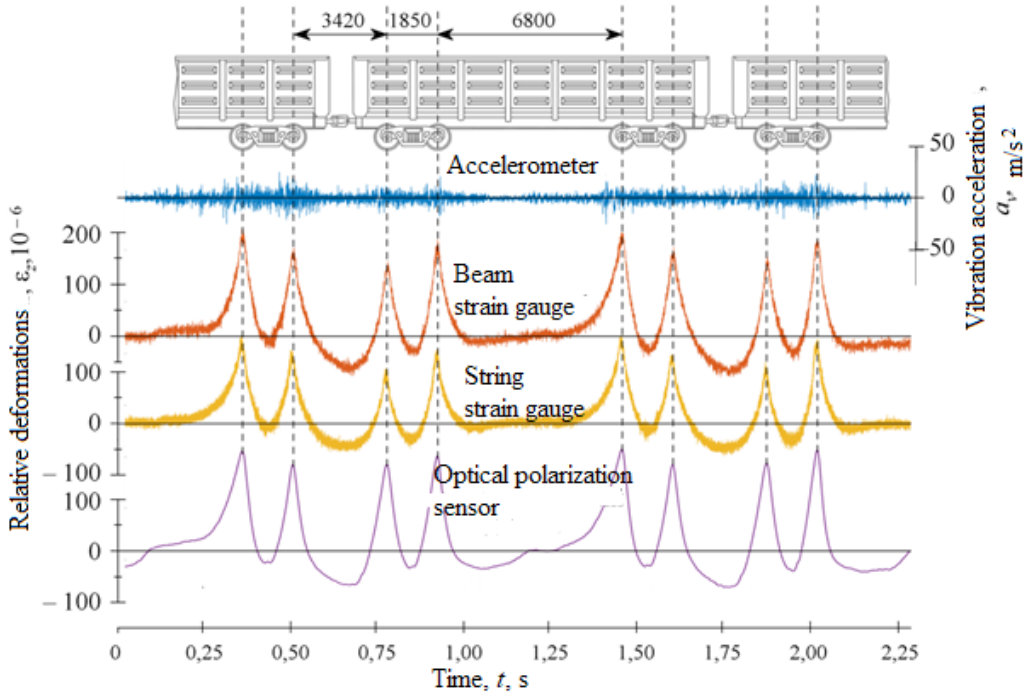

Pic. 5. Diagram of the wheel arrangement of three wagons of a cargo train and the corresponding signals from the accelerometer, beam and string strain gauges, and optical polarisation sensor when eight wheelsets pass (performed by the authors].

track. In the experimental data in Pic. 5, the distance between the measurement points was 2,5 m. Rail deformations depend both on the dynamics of the rolling stock and on the state of the under-rail foundation: stiffness and unevenness along the length of the track; the same statement is true for accelerometer signals.

The verification of relation (8) was performed by double numerical integration of the accelerometer signal and strain gauge signals (Pic. 6). The Pearson correlation coefficient, calculated from local maxima and minima of primitive deformations and vibration acceleration, is greater than 0,99. The similarity of the shape of the second antiderivatives (Pic. 6) and the strong correlation between the extreme values confirm the validity of the integral equation (8), relating vertical vibration acceleration to longitudinal deformations of the foot. When performing numerical integration, the constancy of the average level must be ensured, which is only possible under conditions of symmetrical sensitivity of the strain gauge to compressive and tensile deformations.

Wheelsets' defects such as skids and gouges increase the dynamic force transmitted from the wheel to the rail. The shape of the signals from the strain gauges and accelerometer is distorted (Pic. 7 *a*). Pulse components *1–9* appear in the signals, each of which corresponds to the impact of a running surface defect, that is of a local deviation of the wheel from the circle, on the rail.

The first 6 pulses *1–6* with a fairly high probability relate to one running surface defect, which was registered several times during successive full rotations of the wheel. The average time between adjacent pulses *1–6* (Table 1) is 0,18 s, which at a speed of 59 km/h corresponds to a distance of 2,950 m, equal to the circumference of a wheel with a diameter of 0,94 m. For the first six pulses, the deviation of the time between them from average (Table 1) does not exceed 3 ms, which is comparable to half the oscillation period of 6 ms.

The strain and vibration acceleration pulses recorded in the test are damped oscillations with a frequency of 74 Hz (Pic. 7 *b, c*). The pulses in the signals of the accelerometer and the string strain gauge are equivalent in shape and frequency content, and the signal-to-noise ratio of vibration acceleration is 1,5–2 times higher than that of the string strain gauge.

In the signals of the beam and optical polarisation sensors, signs of slipping of magnetic fasteners along the surface of the rail are observed indicated by a shift in the average

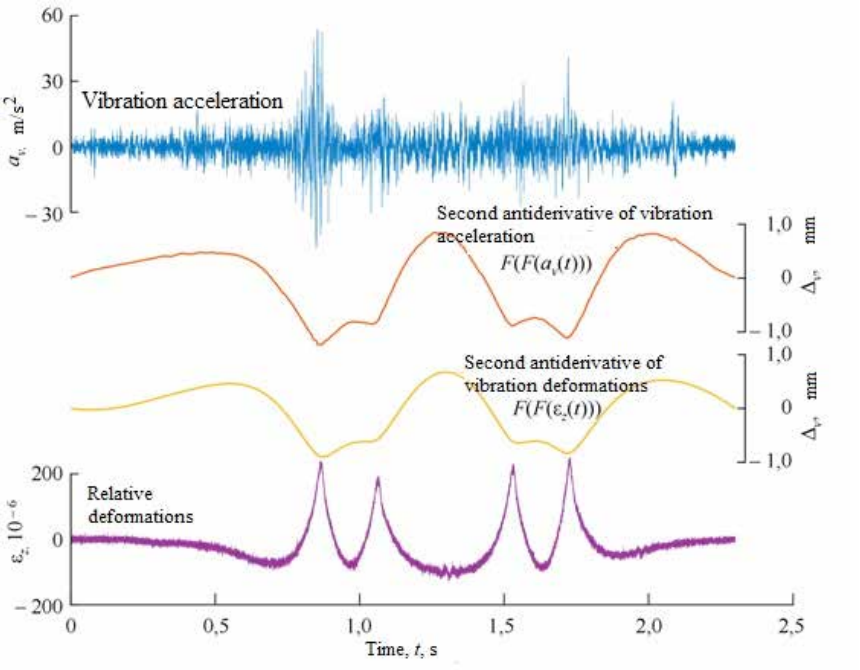

Pic. 6. Signals of the accelerometer $a_y(t)$ and string-type strain gauge $\varepsilon_z(t)$ and their second antiderivatives which are equal to the vertical displacement of the rail base $\Delta_y(t)$ [performed by the authors].

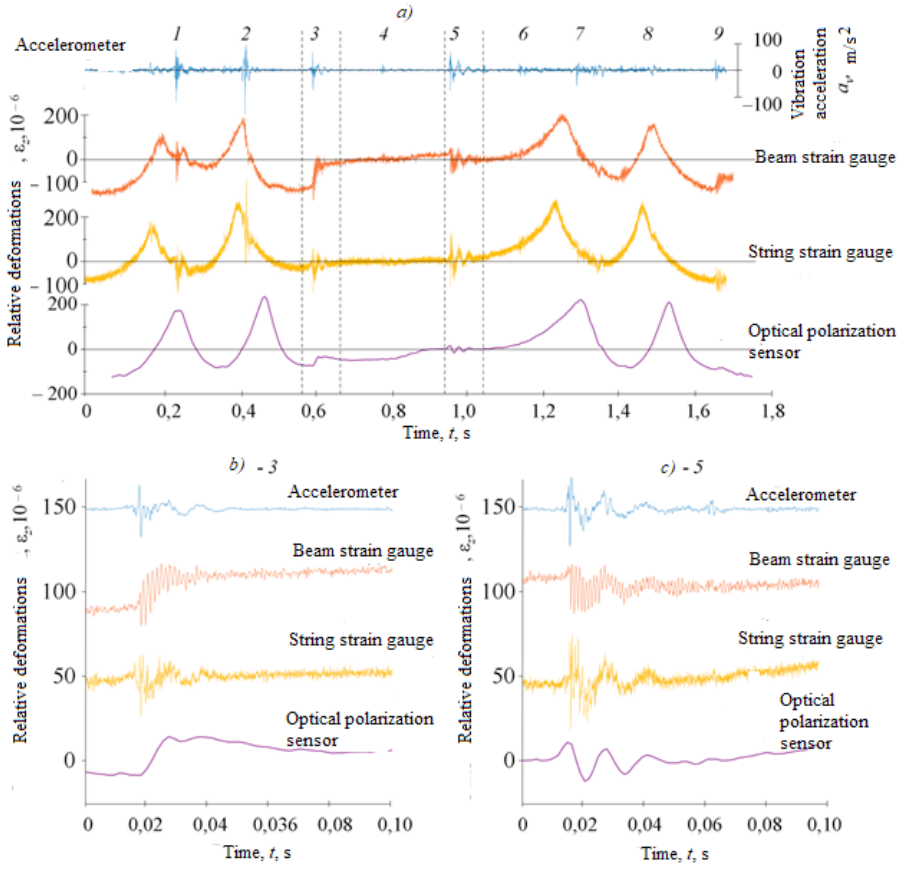

Pic. 7. Signals of the accelerometer $a_y(t)$ and strain gauges $\varepsilon_z(t)$ versus time during the passage of four wheelsets with defects (a) and enlarged fragments of signals with pulses from defects 3 (b) and 5 (c): 1–9 – signal pulses from defects [performed by the authors].

Table 1

Time between vibration acceleration pulses in Pic. 7

Pulse numbers	1–2	2–3	3–4	4–5	5–6	6–7	7–8	8–9
Time between pulses, ms	180	177	180	178	182	151	194	165
Absolute deviation from the average, ms	0,3	-2,2	0,4	-1,6	3,0	-29	15	-15
Relative deviation from the average, %	0,2	-1,2	0,2	-0,9	1,7	-15,9	8,4	-8,2

signal value (Pic. 7 *b*). The spectral composition of these signals is distorted: in the pulse of the beam sensor, a natural oscillation frequency of 800 Hz is observed, and in the optical polarisation sensor there are no frequencies above 200 Hz. All this is due to the designs of the sensors and their fairly large masses, 2–3 times the mass of the string sensor. When a wheel with a defect moves, the massive strain gauge is affected by dynamic forces that exceed the frictional forces and disrupt the fixed contact of the magnetic holders with the rail surface.

KEY FINDINGS AND CONCLUSION

To organise monitoring of the dynamics of vertical depression and longitudinal mechanical stresses of the rail foot during movement of defect-free wheels, both strain sensors and accelerometers can be used. The second antiderivatives in time from vertical acceleration and from longitudinal deformations of the base with constant coefficients are equal to the vertical depression of the rail. This pattern, formulated for a beam model on an elastic foundation, is confirmed by finite element modelling and numerical integration of signals from accelerometers and strain gauges installed on the operating track.

Pulse signals caused by passage of wheels with running surface defects, recorded by accelerometers, have a 1,5–2 times higher signal-to-noise ratio compared to strain gauges. This effect does not impose restrictions on the use of strain gauges since it can be compensated by the use of filtering at the stage of post-processing of digital signals. When a wheelset with a defect on the running surface moves, pulse signals are recorded multiple times, up to six times. The amplitude of the pulses depends on the local stiffness of the under-rail foundation which requires the use of several transducers to unambiguously identify a defective wheelset.

The shape of the recorded pulse components when using magnetic mounts is significantly influenced by the mass, quality factor and natural frequency of strain gauges. Reliable conversion of pulse components by removable strain gauges depends on their mass, which determines the level of dynamic forces.

The results can be used to improve the design and software of stationary diagnostic tools for rolling stock in terms of the level of dynamic impact on the track, increase the reliability of the results and expand their functionality.

REFERENCES

1. Krasnov, O. G., Bogdanov, O. K., Akashev, M. G. Dynamic forces and processes in the rails under impact interaction of wheels with defects. *Russian Railway Science Journal*, 2016, Vol. 75, Iss. 6, pp. 354–364. EDN: XCCLWT.

2. Pevzner, V. O., Petropavlovskaya, I. B., Tretyakov, V. V. [*et al*]. Comparative analysis of the impact on the track of wagons with different axial loads [*Sravnitelniy analiz vozdeistviya na put vagonov s razlichnymi osevymi nagruzkami*]. *Introduction of modern structures and advanced technologies into track management*, 2016, Vol. 9, Iss. 9 (9), pp. 68–75. EDN: WIMBQP.

3. Abdurashitov, A. Yu., Yurkova, Yu. N. On the interaction of track and rolling stock on high-speed traffic sections depending on the outline of the rail and wheel profiles [*O vzaimodeistvii puti i podvizhnogo sostava na uchastkakh skorostnogo dvizheniya v zavisimosti ot ochertaniya profilei relsov i koles*]. *Modern technologies. System analysis. Modeling*, 2022, Iss. 1 (73), pp. 170–177. DOI: 10.26731/1813-9108.2022.1(73).170-177. EDN: CICMUB.

4. Kruglov, V. M., Khokhlov, A. A., Savrukhin, A. V. Model of Dynamic Interaction of Rolling Stock and Track [*Model dinamicheskogo vzaimodeistviya podvizhnogo sostava i puti*]. *World of Transport and Transportation*, 2011, Vol. 9, Iss. 5 (38), pp. 8–11. EDN: OKMCQP.

5. Krasnov, O. G., Efimenko, A. V., Akashev, M. G. The influence of defects on the wheel running surface on the service life of the side frames of cargo wagons [*Vliyanie defektov na poverkhnosti kataniya koles na resurs bokovykh ram gruzovykh vagonov*]. *Vagony i vagonnoe khozyaistvo*, 2014, Iss. 2 (38), pp. 45–48. EDN: SEQIZX.

6. Increasing the reliability and service life of wheelsets and rails [*Povyshenie nadezhnosti i sroka sluzhby kolesnykh par i relsov*]. *Zheleznie dorogi mira*, 2011, Iss. 3, pp. 54–61. EDN: NUGVEZ.

7. Kogan, A. Ya. Impact on the track of trains containing wagons with sliders on wheelsets [*Vozdeistvie na put poezdov, imeyushchikh v svoem sostave vagony s polzunami na kolesnykh parakh*]. *Bulletin of the Scientific Research Institute of Railway Transport*, 2014, Iss. 3, pp. 3–8. EDN: TOLHCB.

8. Zakharov, S. M., Pogorelov, D. Yu., Simonov, V. A. Analysis of the influence of carriages and track parameters on the wear rate in the wheel–rail system (based on a full factorial experiment) [*Analiz vliyaniya parametrov ekipazhei i puti na intensivnost iznosa v sisteme koleso-rels (na osnove polnogo faktornogo eksperimenta)*]. *Bulletin of the Scientific Research Institute of Railway Transport*, 2010, Iss. 2, pp. 31–35. EDN: MEGPGL.

9. Bondarev, E. S. Forecasting the technical condition of rails based on statistical data [*Prognozirovanie tekhnicheskogo sostoyaniya relsov po statisticheskim dannym*]. *Bulletin of the Siberian State Transport University*, 2021, Iss. 4 (59), pp. 55–61. DOI: 10.52170/1815-9265_2021_59_55. EDN: HLDMQB.

10. Makhutov, N. A., Kossov, V. S., Oganyan, E. S., Volokhov, G. M., Ovechnikov, M. N., Protopopov, A. L. Prediction of contact-fatigue damage to rails using computational-experimental methods. *Industrial laboratory. Diagnostics of materials*, 2020, Vol. 86, Iss. 4, pp. 46–55. DOI: 10.26896/1028-6861-2020-86-4-46-55. EDN: UXMYMI.

11. Gromakov, M. S., Tarmaev, A. A., Bespalko, S. V. An energy criterion for estimating the remaining wheel stability from the rolling of the flange onto the railhead during the motion of a wheelset along a straight section. *Modern technologies. System analysis. Modeling*, 2021, Iss. 1(69), pp. 104–111. DOI: 10.26731/1813-9108.2021.1(69).104-111. EDN: DIETDK.

12. Markov, A. A., Maksimova, E. A., Antipov, A. G. Analysis of the development of rail defects based on the results of multi-channel periodic monitoring [*Analiz razvitiya defektov relsov po rezultatam mnogokanalnogo periodicheskogo kontrolya*]. *Defektoskopiya*, 2019, Iss.12, pp. 3–15. DOI: 10.1134/S0130308219120017. EDN: CQVYYL.

13. Markov, A. A., Maksimova, E. A. Analysis of effectiveness of ultrasonic and magnetic channels of flaw detection systems when inspecting rails [*Analiz effektivnosti ultrazvukovykh i magnitnykh kanalov defektoskopicheskikh kompleksov pri kontole relsov*]. *Vestnik IzhGTU imeni M. T. Kalashnikova*, 2019, Iss. 2, Vol. 2, pp.22–32. EDN: HNQVES.

14. Boronenko, Yu. P., Rahimov, R. V., Grigoriev, R. Yu., Popov, V. V. Analysis of methods for measuring the force effect of rolling stock on the track and the wheel control systems when the train is moving. *Izvestiya Peterburgskogo universiteta putei soobshcheniya*, 2020, Vol. 17, Iss. 3, pp. 324–344. DOI: 10.20295/1815-588X-2020-3-324-344. EDN: PDIIKB.

15. Markov, A. A., Maksimova, E. A., Antipov, A. G. Dynamic correction of sensitivity of flaw detection channels during high-speed rail inspection [*Dinamicheskaya korrektsiya chustvitelnosti defektoskopicheskikh kanalov pri vysokoskorostnom kontrole relsov*]. *Defektoskopiya*, 2021, Iss. 12, pp. 3–14. DOI: 10.31857/S0130308221120010. EDN: VMRTBG.

16. Korzhin, S. N., Mironenko, O. I., Melanin, V. M., Bespalko, S. V. Determination of the stress state of a freight wagon wheel from the reaction of the rail [*Opredelenie napryazhennogo sostoyaniya kolesa gruzovogo vagona ot reaktsii relsa*]. *Nauka i tekhnika transporta*, 2021, Iss. 4, pp. 8–12. DOI: 10.53883/20749325_2021_04_08. EDN: FCPDYF.

17. Boronenko, Yu. P., Tretyakov, A. V., Zimakova, M. V. Digital software and hardware platform for automated monitoring of the technical condition of rolling stock and the railway track while the Rubezh train is running [*Tsifrovaya programmno-apparatnaya platform dlya avtomotizirovannogo monitoring tekhnicheskogo sostoyaniya podvizhnogo sostava i zheleznodorozhnogo puti na khodu poezda Rubezh*]. *Proceedings of scientific-practical conference of JSC VNIIZhT «Science 1520 VNIIZhT: Look beyond the horizon» (26–27 August 2021)*. Shcherbinka, JSC VNIIZhT, 2021, pp. 38–44. EDN: OEVRPB.

18. Boronenko, Yu. P., Rakhimov, R. V., Petrov, A. A. Piecewise continuous measurement of forces between the wheel and the rail using shear stresses in two sections of the rail [*Kusochno-nepreryvnoe izmerenie sil mezhdu kolesom i relsom po kasatelnym napryazheniyam v dvukh secheniyakh relsa*]. *Transport Rossiiskoi Federatsii*, 2018, Iss. 3 (76), pp. 58–64. EDN: XRLKOD.

19. Romen, Yu. S., Suslov, O. A., Balyaeva, A. A. Determination of interaction forces in the wheel-rail system based on measuring stresses in the rail web [*Opredelenie sil vzaimodeistviya v sisteme koleso-rels na osnovanii izmereniya napryazhenii v sheike relsa*]. *Bulletin of the Scientific Research Institute of Railway Transport,* 2017, Vol. 76, Iss. 6, pp. 354–361. DOI: 10.21780/2223-9731-2017-76-6-354-361. EDN: YKHKDN.

20. Kossov, V. S., Gapanovich, V. A., Lunin, A. A. [*et al*]. On the issue of determining lateral forces in heavy traffic conditions [*K voprosu opredeleniya bokovykh sil v usloviyakh tyazhelovesnogo dvizheniya*]. *Zheleznodorozhniy transport*, 2018, Iss. 5, pp. 46–51. EDN: XMGKWD.

21. Manshin, Yu. P., Manshina, E. Yu., Geue, M. About the dynamic error of strain gauge torque measuring devices. *Journal of Physics: Conference Series*, Volume 2131, Mathematical modeling and computational methods in problems of electromagnetism, electronics and physics of welding, 052041. DOI: 10.1088/1742-6596/2131/5/ 052041.

22. Dobrovolsky, P. P., Kremis, I. I., Fedorinin, V. N., Sidorov, V. I. Comparative Analysis of the Frequency Responses of Vibration of Rotary Type Microcryogenic Machines. *Optoelectronics, Instrumentation and Data Processing*, 2021, Vol. 57, Iss. 2, pp. 202–207. DOI: 10.3103/S8756699021020060. EDN: ZYTNZV.

23. Sychev, V. P., Shabalin, N. G., Loktev, A. A. [*et al*]. Calculation of the vibration impact on the track of passenger trains at high speeds to ensure safety and comfort of passengers and train crews [*Raschet vibratsionnogo vozdeistviya na put passazhirskikh poezdov s povyshennymi skorostyami dvizheniya dlya obespecheniya bezopasnosti i komfortnosti passazhirov i poezdnykh brigad*]. *Nauka i tekhnika transporta*, 2020, Iss. 3, pp. 110–115. EDN: IHCSZB.

24. Ma, Z., Chung, J., Liu, P., Sohn, H. Bridge displacement estimation by fusing accelerometer and strain gauge measurements. *Structural Control and Health Monitoring*, 2021, Vol. 28, Iss. 6, e2733. DOI: https://doi.org/10.1002/stc.2733 [restricted access].

25. Fedorinin, V. N. Patent No. 2157513 C1 Russian Federation, IPC G01J 4/04. Ellipsometric sensor: No. 99104550/28: appl. 05.03.1999: publ. 10.10.2000; applicant: Design and Technological Institute of Applied Microelectronics SB RAS. EDN: QDFVXB.

26. Kucheryaviy, V. I., Milkov, S. N. Reliability of a gas and oil pipeline in linearly elastic soil during bending [*Nadezhnost gazonefteprovoda v lineino uprugom grunte pri izgibe*]. *Problems of mechanical engineering and machine reliability,* 2017, Iss. 2, pp. 125–130. EDN: YKVAXB. ●

Information about the authors:

Adadurov, Aleksandr S., *Ph.D. (Eng), General Director of VNIIZHT-Engineering Ltd., St. Petersburg, Russia, a.adadurov@vniizht-e.ru.*

Fedorinin, Victor N., *Ph.D. (Eng), Leading Engineer of the Branch of the Rzhanov Institute of Semiconductor Physics of the Siberian Branch of the Russian Academy of Sciences, Novosibirsk, Russia, fedorinin55@mail.ru.*

Bekher, Sergey A., *D.Sc. (Eng), Associate Professor, Professor at the Department of Physics, Electrical Engineering, Diagnostics and Control in Technical Systems of Siberian State Transport University, Novosibirsk, Russia, behers@mail.ru.*

Gulyaev, Mikhail A., *Ph.D. student at Siberian State Transport University, Novosibirsk, Russia, lokigulyaev@gmail, com.*

Article received 03.07.2023, approved after reviewing 30.09.2023, accepted 04.10.2023.